Equilibrium shape degeneracy in starfish vesicles

Xavier Michalet*
Chemistry & Biochemistry Department, UCLA, 607 Charles E. Young Drive East, Los Angeles, California 90095, USA
(Received 30 April 2007; published 10 August 2007)

Phospholipid dispersed in aqueous buffer above their critical micellar concentration form bilayers, which can spontaneously adopt closed metastable shapes with sizes ranging from a few hundred nanometers to few tens of micrometers. The equilibrium shapes of these vesicles are well described by the Canham-Evans-Helfrich curvature elastic energy. Their floppiness allows for thermal fluctuations to be easily detected, but no spontaneous shape transformation is usually observed for vesicles of spherical topological genus (i.e., shapes with no holes) because of strict geometrical constraints and/or energy barriers. This report shows that for a particular class of shapes with spherical topological genus (starfish vesicles), dramatic spontaneous shape transformations can occur due to the degeneracy of the shape solutions, as demonstrated by numerical calculations. These predictions are supported by experimental observations of a three-arm starfish vesicle undergoing spontaneous shape transformations similar to those predicted numerically.

DOI: 10.1103/PhysRevE.76.021914 PACS number(s): 87.16.Dg

I. INTRODUCTION

The theory of equilibrium shapes of closed fluid bilayer membranes (also referred to as vesicles or liposomes) has been established some 30 years ago [1–3] and verified by numerous experimental observations since then (for reviews see, for instance, Refs. [4–6]). Although the focus of modern membrane biophysics has shifted from simple single-component bilayer structures to multicomponent, decorated, scaffolded and/or out of equilibrium structures, to become more relevant for understanding biological structures or for the development of new materials [7], simple systems are always a good starting point to explore fundamental properties. The purpose of this article is to explore a very simple property of some vesicles, the existence of *continuous* families of closed bilayer vesicles with identical curvature elastic energy but widely different shapes. Such degenerate families of shapes have been observed in the past for vesicles of nonspherical topological genus, i.e., vesicles whose shape can be continuously deformed into a sphere with one or more handles (for instance a doughnut shape vesicle has a topological genus 1, as it can be deformed into a sphere with one handle) [8,9]. More precisely, this degeneracy of the equilibrium shape solution was supposed to require a topological genus 2 or larger [10,11]. Although some biological membrane structures such as mitochondria or cell nuclei have nonspherical topologies, the importance of this type of observation remained largely theoretical. The demonstration that such a property also applies to some shapes of topological genus 0 (spherical genus), resulting in dynamics shape changes formally reminiscent of amoeboid motion or pseudopod growth and retraction [12], will hopefully generate further exploration of its relevance for biological and/or technological questions.

The article is organized as follows. The first section will briefly summarize the theory of equilibrium shape of vesicles under geometrical constraints, and discuss the concept of shape degeneracy. Sections II–IV will present some background information on starfish vesicles, describe numerical studies of shape degeneracy in a special case of starfish vesicle and present experimental observations of an example of such shape degeneracy. Section V concludes the article with a brief discussion.

II. EQUILIBRIUM SHAPES OF FLUID VESICLES

The fluidity of bilayers prevents any shear stress to build up in the membrane leaving only two relevant deformations: stretching and bending deformations. The large stretching modulus of fluid membranes sets the energy cost of any significant deviation from the equilibrium area molecular density to values much larger than the thermal energy scale relevant in the present discussion, essentially fixing the surface area of the vesicles [13]. Therefore, only the curvature (or bending) elastic energy is relevant to account for vesicle shapes in the absence of any applied stress. The curvature elastic energy F can be expressed as an integral over the whole surface,

$$F = \frac{\kappa}{2} \oiint dA(2H)^2, \tag{1}$$

where κ is the bending rigidity modulus and the local mean curvature $H=\frac{1}{2}\left(\frac{1}{R_1}+\frac{1}{R_2}\right)$ is defined in terms of the principal radii of curvature of the surface, R_1 and R_2. The bending rigidity modulus has the dimension of energy, and is typically of the order of 10–20 times the thermal energy, k_BT [6]. This explains the spontaneous thermal fluctuations easily observed in the microscope, affecting the average shape of vesicles [14]. Notice that we do not discuss here the contribution F_G of the Gaussian curvature $G=\frac{1}{R_1R_2}$ to F, $F_G=\frac{\kappa_G}{2}\oiint dAG$ as it is a topological invariant [6], and shape transformations discussed in the article will conserve topological genus.

In addition to the conserved surface area (A), two other geometrical parameters appear sufficient to fully describe the variety of observed shapes over typical observation time

*michalet@chem.ucla.edu

scales ($\sim$1 hour): the vesicle volume (V) and area difference (ΔA). The latter is defined as the area difference between the outer and the inner monolayer, and its conservation is due to the negligible exchange of material between the two bilayer's leaflets during observation. Similarly, the aqueous volume enclosed in a vesicle is conserved due to the low permeability of bilayer membranes to water.

The equilibrium shapes of vesicles can be determined by minimization of the curvature elastic energy F under constraints of fixed volume, surface area, and area difference between the two leaflets of the membrane bilayer. Because the curvature elastic energy F is scale invariant, the exact size of the vesicle under study (typically from a few hundred nanometers to a few tens of micrometers) does not matter, and the equilibrium (or minimal) shape is thus defined by a scale R and two dimensionless parameters, the reduced volume v and the reduced mean curvature m related to the area difference ΔA by

$$R = (A/4\pi)^{1/2}, \tag{2}$$

$$v = \frac{3V}{4\pi R^3}, \tag{3}$$

$$m = \Delta A/(2dR) = M/R, \tag{4}$$

where d is the bilayer thickness and M is the integrated mean curvature ($M = \oiint dAH$). Inversely, v and m can be used to define any equilibrium shape up to a scaling factor.

Minimization of F [Eq. (1)] under constraints is performed using Lagrange multiplier for each constraint (V, A, and M) and can be carried out analytically in some limited cases only. Many solutions have been obtained by solving the fourth-order partial differential equation to which the Lagrange equation reduces in the case of axisymmetric shapes [6]. The stability of such solutions with respect to infinitesimal perturbations of the calculated solutions needs to be verified, unstable solutions indicating that nonaxisymmetric solutions are to be looked for. Nonaxisymmetric solutions require a finite elements approach to model the three-dimensional geometry of the vesicles and a direct numerical minimization of the discretized energy, which has been done successfully for different topologies [9,10,15–18]. The end product of this tedious exploration of the shape phase space is a phase diagrams in the (v,m) parameter space, describing the most stable shapes as a function of the constraints [6].

III. METASTABLE SHAPES AND SHAPE DEGENERACY

A shape phase diagram hides the fact that, in addition to absolute minima of F [under constraints (v,m)], many relative minima of F with identical geometrical parameters are the solution of the constrained minimization problem. One defines the shape with minimum energy as the "stable" one and all others as "metastable" ones, although metastable shapes are perfectly stable with respect to infinitesimal perturbations (being solutions of the problem as defined in the previous section).

Metastable shapes cannot transform into the stable one because of the large bending energy cost required to continuously transform the former into the latter, although this barrier can be overcome by thermal energy alone in some specific cases where the barrier is sufficiently low [19]. The existence of these barriers makes "metastable" shapes extremely stable in practice and perfectly observable, provided they can be generated during the vesicle formation process. Such metastable shapes have indeed been experimentally observed for spherical [16] and nonspherical topological genera [9]. In this respect, studying metastable solutions of the minimization problem is experimentally relevant, although the vesicle formation processes which yield metastable shapes remains a highly uncontrolled one and there is currently no practical way to willingly obtain a specific shape experimentally.

What makes the problem of the minimization of F under constraints even more complex is the existence not only of metastable states, but in some cases of degenerate minima of F. Two different situations may occur: (i) these minimal solutions are separated by energy barriers in the shape phase space, or (ii) these solutions belong to a continuous family of solutions (not separated by energy barriers). The first situation has been described in a few cases for shapes of spherical topological genus [16,19] and will be discussed in more detail in the next section. Examples where the second kind of degeneracy occurs have been presented both theoretically [10,11] and experimentally [8,15] in the case of shapes of topological genus larger than 1. In these cases of degenerate minima, no shape is more probable than another, and a continuous, random exploration of the whole shape family is experimentally observed, with a typical time scale of several minutes, which markedly distinguishes it from mere shape fluctuations. Up to now, these zero-energy mode shape transformations have only been predicted and observed for shapes with more than one hole (topological genus larger than 1).

IV. STARFISH VESICLES

A. Basic facts and a conjecture

In an esthetically fascinating report, Wintz *et al.* described several starfishlike vesicles whose shapes they could reproduce by numerical minimization of the curvature elastic energy [16]. Among this class of shapes, initially reported by Hotani [20], they showed that several different shapes exist having the same energy, but characterized by different symmetry groups. These shapes are all solutions of the minimization problem under the same geometrical constraints and very stable. In particular, no transformation from one shape to another was observed experimentally. As discussed previously, this can be attributed to energy barriers separating the different minima of the curvature elastic energy that thermal energy alone cannot overcome. Another recent report [18], has identified starfish vesicles as the most stable equilibrium shapes in a region of the phase diagram with larger reduced volume v $(0.5<v<0.6)$ than those reported by Wintz *et al.* $(0.3<v<0.5)$. Quoting Ref. [16], all these shapes can be qualitatively described as "built up using three structural elements. The center consists of a quite flat, nearly axisymmet-

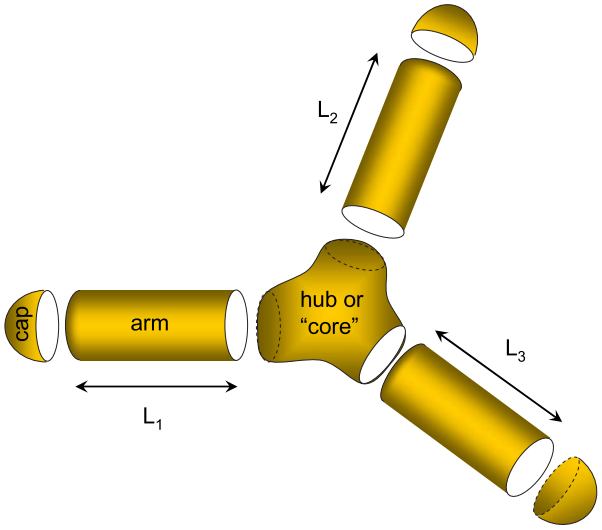

FIG. 1. (Color online) Schematic decomposition of starfish shapes in terms of cylinder sections, caps and hub.

ric *core*. Attached to this core are *cylindrical arms* which end in *spherical caps*. The radius of the caps is somewhat larger than the radius of the cylinder. The overall shape is quite flat." Fig. 1 illustrates this construction principle for a three-arm starfish vesicle. Note that such shapes are also observed in multicomponent vesicles [21]. To obtain a qualitative idea of the geometric characteristics of these shapes, we shall consider shapes consisting of n very long cylindrical arms of total length L and diameter $d<L$. For long enough arms, the contribution of the core and the caps to the total volume and area will be negligible, and the approximate reduced volume of such shapes will be

$$v \sim \frac{3}{2}\left(\frac{d}{L}\right)^{1/2}. \tag{5}$$

Similarly, the mean reduced curvature of such shapes is given by

$$m \sim 2\pi\left(\frac{d}{L}\right)^{-1/2}, \tag{6}$$

and its curvature elastic energy by

$$F \sim 2\pi\kappa\left(\frac{d}{L}\right)^{-1}. \tag{7}$$

As a reminder, the curvature elastic energy of a sphere is $8\pi\kappa$. Starfishs with $v=0.3$ thus correspond to $d/L\sim 0.04$, $m\sim 2.5\times 4\pi$, and $F\sim 6.25\times 8\pi\kappa$. Shapes with smaller d/L ratio correspond to a region of the phase diagram that remains to be investigated as far as nonaxisymmetric shapes are concerned.

The simple description of starfish vesicles of small aspect ratio d/L as a series of n closed tubular sections connected to a small hub region suggests that in the limit of very long tubular sections, the exact length L_i of each tubular section i should not matter much, the total length $L=\Sigma L_i$ being the only parameter entering Eqs. (5)–(7) (with the additional parameter d). In other words, we can conjecture that there might be an infinite number of families of starfish vesicles $\{n,v,m\}$ with n arms of variable lengths $\{L_i\}$ but equal total length L having identical geometrical parameters (v,m) and energy F. Since the transformation from one such hypothetical starfish vesicle $\{L_i\}$ of a given family to an infinitesimally close one $\{L_i,\ldots,L_k-\delta L,\ldots,L_p+\delta L,\ldots L_n\}$ consists in a simple exchange of lipids from one arm (k) to the other (p), there should be no curvature elastic energy barrier to this transformation and all shapes belonging to a given family $\{n,v,m\}$ should be able to continuously transform into one another.

B. Numerical study of shape degeneracy in starfish vesicles

The previous simple approximation of the shape of starfish vesicles neglects the contribution of the caps and hub to v and m and ignores the likely departure of the arm shapes from exact cylinders. Any minute changes in shape could result in a non-negligible change in curvature elastic energy, and invalidate the previous conjecture. A simple and necessary test therefore consists in performing a direct minimization of the curvature elastic energy under constraints.

The SURFACE EVOLVER is a convenient software to do this. Developed by Brakke [22,23], it is freely available [32], and has been successfully used for various vesicle shape calculations [8,9,15,17,18] among other applications. It is straightforward to define triangulated surfaces approximating three-arm starfish vesicles. Figure 2 shows an example of a starting surface used in the calculations described here. It consists in 18 vertices, 27 edges (segment connecting two vertices), and 11 facets (list of oriented edges). An example SURFACE EVOLVER file is provided in Ref. [31]. The volume V, area A, and mean integrated curvature M were computed and set as constraints for the minimization. Each surface was then "evolved" to minimize the curvature elastic energy F using SURFACE EVOLVER. The SURFACE EVOLVER "evolves" the surface toward minimal energy by a gradient descent method, moving each vertex by a multiple of the force applied to this vertex [22]. In a second phase, the constraints were changed stepwise to reach the target values of the surface family. After each constraint modification, the surfaces were evolved to minimize F. Finally the shapes were progressively refined and evolved to minimize the curvature elastic energy under the target constraints.

Since F is scale invariant, the length scale is arbitrary. To fix the ideas, let us set $L=21$ and $d=1$ (arbitrary units). The most symmetric starfish of the family is given by $L_1=L_2=L_3=7$. To keep the number of calculations manageable, only members of the family with integer arm length were considered. Shapes with initial arm size smaller than 3 were not stable. This leaves only 19 members with initial integer arm size $(L_1,L_2,L_3)=[i,j,(21-i-j)]$ with $(3\leq i,j\leq 9)$, as listed in Table I. All these shapes were calculated to a final resolution of $\sim 10\,000$ facets and evolved until a stable energy was obtained. Examples of these solutions with a common reduced volume $v=0.297$ and reduced mean curvature $m=2.269\times 4\pi$ are represented in Fig. 3. The stability of the shapes was tested by small random perturbations applied

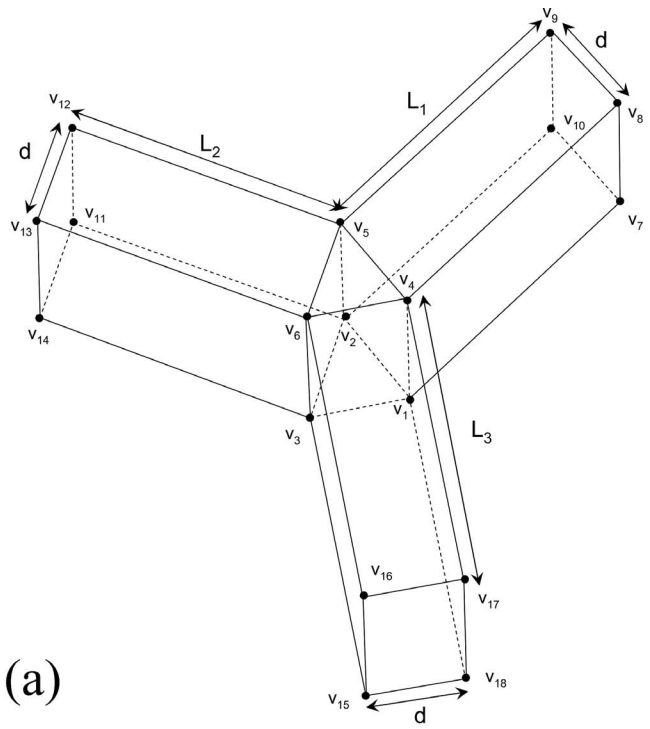

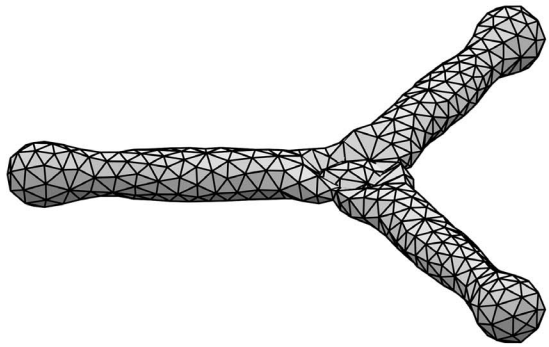

(b)

FIG. 2. (a) Starting point for the SURFACE EVOLVER calculations consisting of 18 vertices, 27 edges, and 11 facets. The vertices definition corresponds to that used in the Evolver file provided in Ref. [31]. (b) Surface after a few rounds of refinement.

globally to the shape, a noteworthy feature of the SURFACE EVOLVER. All shapes converged back to their previous minimum. Although only the initial geometry and the constraints were fixed, all 19 shapes ended up having a similar energy

TABLE I. Sets of starfish arm length $(L_1,L_2,L_3)=[i,j,21-(i+j)]$ used in the reported calculation.

3, 3, 15	3, 4, 14	3, 5, 13	3, 6, 12	3, 7, 11	3, 8, 10	3, 9, 9
4, 4, 13	4, 5, 12	4, 6, 11	4, 7, 10	4, 8, 9		
5, 5, 11	5, 6, 10	5, 7, 9	5, 8, 8			
6, 6, 9	6, 7, 8					
7, 7, 7						

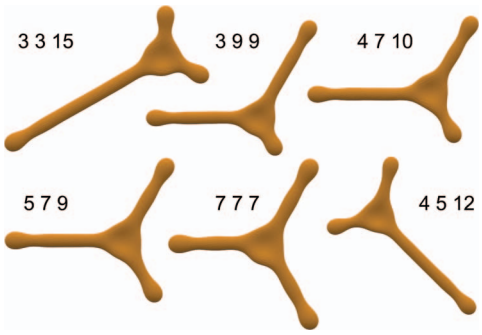

FIG. 3. (Color online) Examples of computed starfish shapes with $v=0.297$, $m=2.269\times 4\pi$. Each shape is labeled with the three-arm lengths: L_1 L_2 L_3 (in arbitrary units). The shapes are composed of $\sim$10 000 facets, and have a similar energy of $6.716(2)\times 8\pi\kappa$.

$F=6.716(2)\times 8\pi\kappa$ which can in fact be considered identical up to the numerical uncertainty of this calculation.

Although limited to a single set of (v,m) values and to a family of $n=3$ arm vesicles, these calculations strongly suggest the validity of the conjecture according to which there exist degenerate families of starfish vesicles in the region of low reduced volume. The practical implication of this prediction is that, should such vesicles be observed, no specific shape within a family is energetically favored, and therefore random exploration of the whole family should take place. Such random exploration can be pictured as a random diffusion in the phase space consisting of all the shapes belonging to a starfish family (n,v,m) such as the one described for higher topological genus shapes [11]. For the case of three-arm starfish vesicles, the numerical calculation confirms that the relevant descriptive parameter of each shape is the three-arm lengths L_1, L_2, and L_3 (constrained by $L_1+L_2+L_3=$ constant), since all arms have an identical diameter and volume is conserved. A simple representation of such a shape is a point located within an isosceles triangle of side $2/\sqrt{3}\times L$ as indicated in Fig. 4. Indeed, the sum of the distances to all three sides is a constant equal to the height of the triangle. Random exploration of the shape family can therefore be represented as a random path within the boundaries of the triangle.

The next section provides experimental evidence of these different predictions.

C. Experimental observation of shape degeneracy in starfish vesicle

Vesicles were formed using standard material and protocols. 1 mg of dimyristoylphosphatidylcholine (DMPC, Avanti Polar Lipids) was hydrated with 10 μl of citrate coated (negatively charged) magnetic particles [24,25] and 500 μl of doubly distilled water (pH$\sim$7). Vesicles spontaneously form after several hours of incubation at room temperature, after which an aliquot was mounted in a sealed observation chamber. Vesicles were observed at room temperature ($\sim$25 °C) with an inverted phase contrast microscope equipped with an $\times$40 objective (Nikon). At this temperature, DMPC bilayers are in the fluid phase [26]. Further

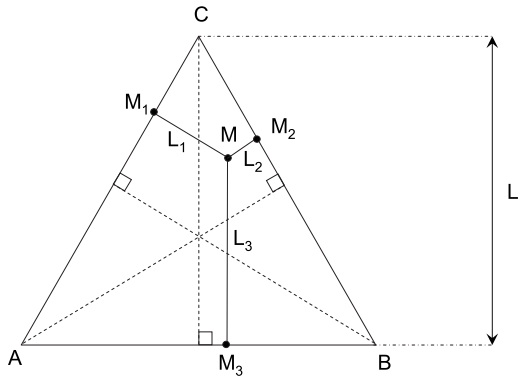

FIG. 4. Schematic representation of the phase space of starfish vesicles of a degenerate family. A point M within the isosceles triangle ABC of side a and height $L=\sqrt{3}/2\times a$ is the summit of three triangles: MAB, MBC, MCA. The respective areas of these triangles are: $\frac{1}{2}MM_3\times AB$, $\frac{1}{2}MM_2\times BC$, $\frac{1}{2}MM_1\times CA$. Their total area $\frac{1}{2}a(MM_1+MM_2+MM_3)$ equals that of the triangle ABC $=\frac{1}{2}aL$. Therefore any point M within the triangle represents a vesicle of arm length $(L_1,L_2,L_3)=(MM_1,MM_2,MM_3)$ with $L_1+L_2+L_3=L$.

magnification was available through a $(\times 0.9-\times 2.25)$ zoom module to which a simple monochrome video charge-coupled device camera was attached. The video was recorded on S-VHS videotapes and later on digitized using a frame-grabber installed in a personal computer.

Vesicles were formed in a dilute ferrofluid solution in the hope that this would permit their manipulation by application of a magnetic field [27]. In practice, the only observable effect of an external magnetic field temporarily applied with the help of a small handheld 1 Tesla magnet in the vicinity of the observation chamber was to create a flow surrounding the vesicles, by which they could be dragged. All the observations described in the following were performed in the absence of a magnetic field, and it is therefore assumed that the minute amount of ferrofluids present in the solution had no bearing on the behavior of the vesicles.

Figure 5 shows a series of phase contrast images of a three-arm starfish vesicle taken from the movie provided as

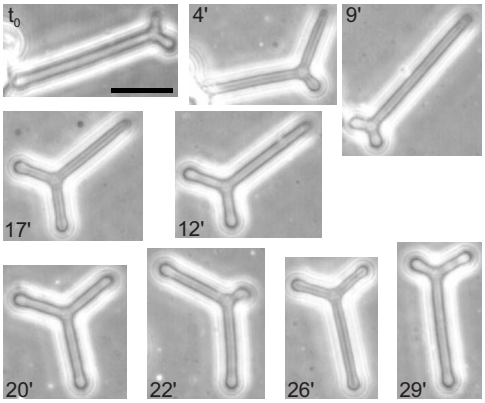

FIG. 5. Series of phase contrast images of a three-arm starfish vesicle. The time after the beginning of observation is indicated in minutes. Scale bar (for all images) represents 20 μm.

supplementary information [31]. Qualitatively, the vesicle shapes appear similar to those described in the previous section and represented in Fig. 3, although the hub diameter is larger in the simulated shapes. This discrepancy is due to the fact that the vesicle does not have the same geometric parameters (v,m) as those chosen for the numerical example described previously. Over time, the arms appear to grow or shrink randomly, while preserving the initial volume of the vesicle and as well as the arms diameter. The typical time scale of the vesicle evolution is several minutes, and can be more fully appreciated by looking at the accelerated movie provided as supplementary information [31].

Following the notations introduced previously, each state of the starfish vesicle can be characterized by the set of three armlengths (their sum total being constant within the experimental uncertainty) and represented in an isosceles triangle in which the "path" of the vesicle can be followed minute by minute (Fig. 6). The evolution is spontaneous and seems random during the observation period, with bouts of faster evolution (as between t_0+24 min and t_0+25 min) or slower one (as in the first 10 minutes).

V. DISCUSSION

A. Numerical results

The numerical results of the previous section are no proof of the exact degeneracy of the curvature elastic energy F but are as close as one can get obtain with this approach from establishing the existence of a continuous family of starfish vesicles with identical geometric parameters (v,m). It is easy to extend these calculations to different sets of parameters using the SURFACE EVOLVER and the source file provided in [31]. In particular, by reducing the aspect ratio d/L, starfish

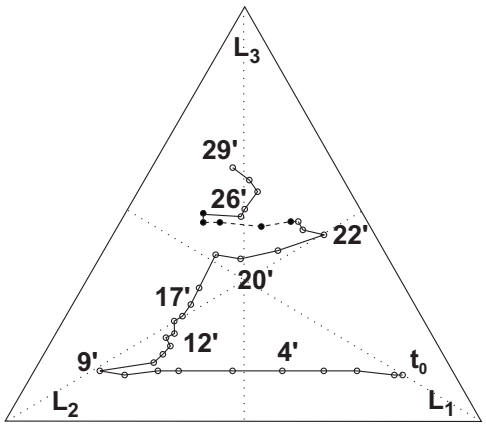

FIG. 6. Path of the starfish vesicle. Each state of the vesicle is defined by the lengths of its three arms, L_1, L_2, and $L_3=L-(L_1+L_2)$, where L is the sum total length and is represented by a circle. For instance, the length of arm 1 (pointing to the lower left, and later on due to rotation, to the upper left in Fig. 5) can be read along the direction of the dashed line marked L_1 as the distance towards the opposite face. The vesicle state is represented every minute, except for a brief period between the 24th and 25th minutes during which the shape evolution accelerated (dashed line), where it is reported every 5 seconds.

surfaces with much lower (and in principle arbitrarily low) reduced volume could be obtained.

As suggested by the calculations of Wintz *et al.* families of starfish vesicles with more than three arms should also be considered and are likely to give similar results as reported here in the limit of long arms (and small aspect ratio). That is, only the total length of all arms matters, and shapes with different sets of arm lengths will turn out to have identical energies F. The extension of the numerical work presented here to larger n does not present any difficulty of principle. Interestingly, starfish shapes considered up to now have been limited to shapes with a plane of symmetry (or "flat" starfish). There does not seem to be any reason why shapes with other groups of symmetry (in the case of the shape with n arms of equal length) or even no symmetry at all would not be stable. The simplest example of such a shape would be a four-arm vesicle with the hub section at the center of a tetrahedron, and arms directed towards the summits. Such "urchin" or echinocyte and/or acanthocyte shapes (which have been computed at much higher reduced volume [17]) would considerably increase the population of low reduced volume shapes of the phase diagram exhibiting shape degeneracy, and do not present any difficulty of principle to study numerically.

B. Experimental results

The experimental observations presented here confirm the relevance of the numerical calculations, predicting the degeneracy of a similar family of three-arm starfish shapes. The identical curvature elastic energy of all shapes is expected to translate in a random exploration of the family, as long as the shape transformation does not involve any other energy cost. In fact, the shape transformations in solution (by opposition to shape transformations *in silico*) involve moving parts of the vesicle through a fluid environment, which should come at an energetic cost due to the viscous drag. It is well known, however, that Brownian rotation and translation of vesicles due to thermal agitation are commonly observed in solution. Therefore thermal energy should be sufficient to overcome the viscous drag on the moving parts of the vesicle, and the observations reported above are consistent with this scenario. A typical time scale τ_{dif} for this motion is obtained by considering the linear Brownian diffusion of a hemispherical cap of diameter d over a distance L (since only the tips of the arms actually move within the fluid). Using the Stokes-Einstein expression for the diffusion coefficient D,

$$\tau_{dif} \sim \frac{L^2}{2D} = \frac{3\pi}{2}\frac{\eta L^2 d}{k_B T}, \tag{8}$$

where η is the fluid viscosity. With $\eta_{water}=0.001$ Pa s, $L=30$ μm, $d=3$ μm, we obtain $\tau_{dif}\sim 52$ min. This value compares qualitatively well with the observed duration of a single arm growth or shrinkage of ~ 10 min. Its order of magnitude is in any case markedly different from the typical time scale τ_{und} of a few seconds for the thermal undulations of a tubular membrane [28,29], which can also be observed in the movie provided as supplementary information [31].

A characterization of the lipid dynamics in the membrane, for instance using fluorescence markers, would allow determining whether the observed time scale and shape transformation involves anything else than pure lipid diffusion. Future experiments may also yield longer trajectories in phase space enabling a better quantification of the randomness of these shape transformations.

C. Perspectives

As discussed previously, the degeneracy of the set of solutions to the minimization problem exhibited here for three-arm starfish vesicles is most likely occurring for $n>$ three-arm starfish vesicles as well and potentially more complex geometries, all characterized by interconnected long tubular sections. Similar geometries occur commonly in live organisms, such as, for instance, in the architecture of the endoplasmic reticulum of mammalian cells or some mitochondria structures. Whereas these structures have sometimes been approached from the three-dimensional minimal surface point of view, they are exactly so only in rare cases [30], the present work suggests that a more disordered description in terms of (closed) interconnected tubules might shed light on their dynamics. Indeed, one of the key points of this description is that some complex interconnected tubular shapes may adopt very different conformations at no curvature elastic energy cost, while maintaining their enclosed volume, surface area, and area difference. In fact, based on previous observations of fluctuating passages between stacks of membranes [8], the common picture emerging from these observations is that a large number of low reduced volume membrane shapes occurring in nature (not necessarily tubular) might belong to families of degenerate minima of the curvature elastic energy. Of course, many biological membranes are multicomponent, decorated with multiple proteins, and in many cases, scaffolded by an underlying protein skeleton, in which cases the simple energy considered here is insufficient to account for their mechanical properties. It will therefore be interesting to study the robustness of this degeneracy in more complex models.

ACKNOWLEDGMENTS

I want to warmly thank David Bensimon (Ecole Normale Supérieure, FR) in whose laboratory I performed the observations reported here. I am grateful to Kenneth Brakke (Susquehanna University, PA) for his SURFACE EVOLVER program and kind support. Valerie Cabuil and Christine Ménager (Université Pierre et Marie Curie, FR) are gratefully acknowledged for providing the ferrofluids.

[1] P. B. Canham, J. Theor. Biol. **26**, 61 (1970).
[2] W. Helfrich, Z. Naturforsch. C **28c**, 693 (1973).
[3] E. A. Evans, Biophys. J. **14**, 923 (1974).
[4] R. Lipowsky, Nature (London) **349**, 475 (1991).
[5] R. Lipowsky, Curr. Opin. Struct. Biol. **5**, 531 (1995).
[6] U. Seifert, Adv. Phys. **46**, 13 (1997).
[7] E. Sackmann, J. Phys.: Condens. Matter **18**, R785. (2006).
[8] X. Michalet, D. Bensimon, and B. Fourcade, Phys. Rev. Lett. **72**, 168 (1994).
[9] X. Michalet and D. Bensimon, J. Phys. II **5**, 263 (1995).
[10] F. Jülicher, U. Seifert, and R. Lipowsky, Phys. Rev. Lett. **71**, 452 (1993).
[11] F. Jülicher, J. Phys. II **6**, 1797 (1996).
[12] L. G. E. Bell and K. W. Jeon, Nature (London) **198**, 675 (1963).
[13] E. Evans and W. Rawicz, Phys. Rev. Lett. **64**, 2094 (1990).
[14] J. F. Faucon *et al.*, J. Phys. (France) **50**, 2389 (1989).
[15] X. Michalet and D. Bensimon, Science **269**, 666 (1995).
[16] W. Wintz, H.-G. Döbereiner, and U. Seifert, Europhys. Lett. **33**, 403 (1996).
[17] Jie Yan, Quan Hui Liu, Ji Xing Liu, and Zhong-can Ou-Yang, Phys. Rev. E **58**, 4730 (1998).
[18] P. Ziherl and S. Svetina, Europhys. Lett. **70**, 690 (2005).
[19] H.-G. Döbereiner and U. Seifert, Europhys. Lett. **36**, 352 (1996).
[20] H. Hotani, J. Mol. Biol. **178**, 113 (1984).
[21] T. Baumgart, S. T. Hess, and W. W. Webb, Nature (London) **425**, 821 (2003).
[22] K. A. Brakke, Exp. Math. **1**, 141 (1992).
[23] K. A. Brakke, Philos. Trans. R. Soc. London, Ser. A **354**, 1243 (1996).
[24] J.-C. Bacri, V. Cabuil, A. Cebers, C. Ménager and R. Perzynski, Math Sci Eng. C **2**, 197 (1995)
[25] R. Massard, IEEE Trans. Magn. **17**, 1247 (1981).
[26] S. L. Keller, A. Radhakrishnan, and H. M. McConnell, J. Phys. Chem. B **104**, 7522 (2000).
[27] O. Sandre, C. Ménager, J. Prost, V. Cabuil, J. C. Bacri, and A. Cebers, Phys. Rev. E **62**, 3865 (2000).
[28] R. M. Servuss, W. Harbich, and W. Helfrich, Biochim. Biophys. Acta **436**, 900 (1976).
[29] M. B. Schneider, J. T. Jenkins, and W. W. Webb, Biophys. J. **45**, 891 (1984).
[30] Z. A. Almsherqi, S. D. Kohlwein, and Y. Deng, J. Cell Biol. **173**, 839 (2006).
[31] See EPAPS Document No. E-PLEEE8-76-176707 for a movie showing the sequence of shape transformations as well as an example Evolver file. For more information on EPAPS, see http://www.aip.org/pubservs/epaps.html.
[32] http://www.susqu.edu/brakke/evolver/evolver.html